Evaluation of the New WAAS L5 Signal

Hyunho Rho and Richard B. Langley
Department of Geodesy and Geomatics Engineering, University of New Brunswick, Fredericton, N.B. Canada

BIOGRAPHY

Hyunho Rho received an M.Sc. in 1999 in geomatics from Inha University, South Korea. He is currently a Ph.D. candidate in the Department of Geodesy and Geomatics Engineering at the University of New Brunswick (UNB), where he is investigating ways to improve ionospheric modeling for wide area differential GPS (WADGPS) and precise point positioning with WADGPS corrections.

Richard Langley is a professor in the Department of Geodesy and Geomatics Engineering at UNB, where he has been teaching since 1981. He has a B.Sc. in applied physics from the University of Waterloo and a Ph.D. in experimental space science from York University, Toronto. Prof. Langley has been active in the development of GPS error models since the early 1980s and is a contributing editor and columnist for GPS World magazine. He is a fellow of the ION and shared the ION 2003 Burka Award. He received the ION's Kepler Award in 2007. He is also a fellow of the Royal Institute of Navigation and the International Association of Geodesy.

ABSTRACT

The current GPS constellation is being modernized to enhance the performance of the legacy GPS signals. As a part of the GPS modernization efforts, a new third civil signal, L5 at 1176.45 MHz will join the current civil signal on L1 at 1575.42 MHz and the second civil signal on L2 at 1227.60 MHz. Since the Wide Area Augmentation System (WAAS) is compatible with the GPS modernization, both WAAS geostationary Earth orbiting satellites (GEOs), Galaxy XV (PRN135) and Anik F1R (PRN138) contain an L1 and L5 GPS payload and currently broadcast both signals on the air.

The main objective of the research described in this paper is the evaluation of the new WAAS L5 signal. In the work reported in this paper, the overall quality of the new WAAS L5 signal was investigated by comparing selected signal quality indices, such as the carrier power to noise density ratio (C/N_0) and multipath plus noise level, between the L1 and L5 signals.

Since WAAS GEO signals are generated by the ground control segment and uplinked to GEOs to broadcast the signals on the air (a so-called "bent-pipe" approach), the ionospheric delays as well as differential code bias (DCB) should be estimated and compensated for in both the uplink and downlink signals. The behavior of the DCB for PRN138 has been further analyzed in this research.

This paper presents the evaluated results for the new WAAS L5 signal quality and the identified WAAS GEO satellite DCBs as well as some discussions about the possible benefit of the WAAS GEO ranging measurements in the positioning domain.

INTRODUCTION

As a part of the GPS modernization efforts, a new third civil signal, L5 at 1176.45 MHz will join the current civil signal on L1 at 1575.42 MHz and the second civil signal on L2 which is also undergoing modernization (L2C), at 1227.60 MHz. This new satellite signal is anticipated to provide better quality range measurements and possibly improve the tracking performance of a GPS receiver compared with current L1 and L2 signals by adopting improved signal structures. This includes using an increased chipping rate of 10.23 megachips per second (Mcps) instead of 1.023 Mcps for L1 C/A (C1) code and a higher transmitted power than L1/L2 signals and a longer spreading code than L1 C1 (see the following Table 1 and Table 2). It will also be beneficial for mitigating the ionospheric error that is currently the largest GPS error source by use of the multiple frequencies of signals for civilian. More detailed descriptions of the L5 signal can be found in Van Dierendonck and Hegarty [2000], Enge [2003] and IS-GPS-705 [2005].

Since the Wide Area Augmentation System (WAAS) should be compatible with GPS modernization, both WAAS geostationary Earth orbiting satellites (GEOs), Galaxy XV (PRN135) and Anik F1R (PRN138) contain an L1 and L5 GPS payload and currently broadcast both signals on the air [Schempp, 2008]. The WAAS L5 signal structure is similar to the GPS L5 signal except that only a single channel carrier is used, and the data rate is increased to 250 bps [Hsu et al., 2004]. The different

signal characteristics of GPS and WAAS are illustrated in Table 1.

Table 1: Characteristics of GPS L5 signal vs. WAAS L5 [IS-GPS-200D, 2004 and IS-GPS-705, 2005]

	GPS L5	WAAS L5	GPS/WAAS L1
Carrier Frequency	1176.45 MHz	1176.45 MHz	1575.42 MHz
Signal Structure	Two carrier components: I5 and Q5 ranging codes	Single carrier component: C5 ranging code	Two carrier components: P(Y) and CA /CA ranging code (WAAS)
Code length (chips)	10230	10230	1023
Code frequency	10.23 Mcps	10.23 Mcps	1.023 Mcps
Data rate	50 bps	250 bps	50/250 bps

Table 2: Received Minimal Signal Strength [IS-GPS-200D, 2004 and IS-GPS-705, 2005]

SV Blocks	Channel	Signal	
		P(Y)	C/A or L2C
II/IIA/IIR	L1	-161.5 dBW	-158.5 dBW
	L2	-164.5 dBW	N/A
IIR-M/IIF	L1	-161.5dBW	-158.5 dBW
	L2	-161.5 dBW	-160.0 dBW
IIF		I5	Q5
	L5	-157.9 dBW	-157.9 dBW

A NovAtel ProPak-V3 (OEM-V3) receiver equipped with specialized firmware that allows acquisition of both L1 and L5 signals simultaneously from the WAAS GEOs was used to obtain test data sets at the University of New Brunswick (UNB) in Fredericton Canada. A data set spanning four continuous days in August 2008 has been used to study the WAAS L5 signals.

This paper discusses the overall observation quality of WAAS L5 signals. Since the carrier power to noise density ratio (C/N_0) indicates the level of signal power versus the level of background noise in the observables, C/N_0 was used as a first signal quality indicator and the C/N_0 values on L1 and L5 signals were compared. Also the receiver tracking noise and multipath (MP) characteristics of the L1 and L5 signals were compared. In this comparison, the magnitude of possible improvement from enhanced signal structures in the L5 signal are quantified.

In the following sections, the WAAS differential code bias (DCB) between L1 C1 and L5 code (C5) are analyzed. Since the WAAS GEO ranging signals are generated by the ground control segment and uplinked to the GEO satellites for rebroadcast [Hsu et al., 2004 and 2007, Grewal, 2008], the ionospheric delays as well as its differential code bias (DCB) should be estimated and compensated for in both the uplink and downlink signals. Since another important role of DCB in WAAS might be to resolve the clock referencing issue in the observables for single frequency users (like the group delay term (T_{GD}) for GPS L1/L2 [IS-GPS-200D]), the overall behavior of the estimated DCBs were further analyzed. Finally, the possible benefit of using WAAS GEO ranging measurements in the positioning domain is also discussed.

In this paper, investigations of the observation quality of the WAAS L5 signal are presented. Furthermore the compiled statistics of all the compared results for the selected continuous four days are presented, which may be used as a baseline for further research on the WAAS and future GPS L5 signals.

OBSERVABILITY OF L5 SIGNALS AT UNB

WAAS currently transmits dual-frequency, L1 and L5 signals on the air. At UNB, the two WAAS GEOs, PRN135 and PRN138 can be simultaneously monitored. Both GEOs are located on the southwest side of UNB and PRN135 is monitored at an elevation angle of 7.6° and azimuth of 252.6°. PRN138 is monitored at an elevation angle of about 23.9° and azimuth of 230.1°. The following Figure 1 shows the observability of signals from the WAAS GEOs at UNB.

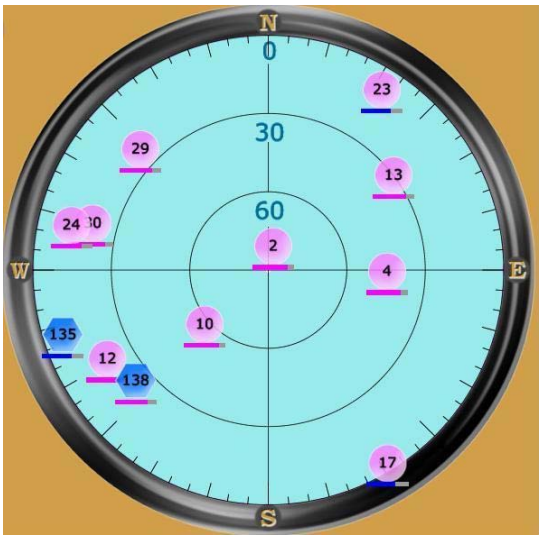

Figure 1. Observability of signals from WAAS GEOs at UNB

To obtain test data sets at UNB, we used a NovAtel ProPak-V3 (OEM-V3) receiver equipped with specialized firmware that allows acquisition of both L1 and L5 signals simultaneously from the WAAS GEOs. The first four channels of the entire sixteen-channel receiver were assigned to the two WAAS GEOs for L1 and L5 dual frequency tracking and the other 12 channels were used for general GPS L1 and L2 dual frequency tracking. With this capability, the observation quality of the WAAS L5 signals could be directly compared with the WAAS L1 signals and the simultaneous GPS dual frequency measurements could be used for other purposes such as comparing the differences of the estimated DCBs for GPS and for WAAS.

Since PRN135 is seen at the low elevation angle of around 7.6°, an elevation cutoff angle of 0° was used to collect data from all satellites. The collected data set for the continuous four days from 24 August 2008 to 27 August 2008 have been used to assess the quality of the L1 C1 and the new L5 C5 code measurements (pseudoranges).

METHODOLOGY

The objective of this section is to describe the computational methods we used to obtain "proper" observables which have been used to evaluate the WAAS L5 signals.

Multipath Plus Noise Observables

At first, pseudorange measurements can be expressed in distance units as:

$$P_i = \rho + c\cdot(dT - dt) + d_{ion,i} + d_{trop} + b^{s_k,Pi} + b_{rj,Pi} + mp_{Pi} \quad (1)$$

where *i* stands for the corresponding frequency at L1, L2 or L5 for satellite k and receiver j, P is the pseudorange measurement in distance units, ρ is the geometric range between the satellite and the receiver, *dT* and *dt* represent the receiver and satellite clock offsets relative to system reference time, i.e. GPS Time for GPS satellites and WAAS network time for WAAS GEOs, $d_{ion,i}$ is the frequency dependent ionospheric delay and d_{trop} *is* the tropospheric propagation delay, $b^{s_k,Pi}$ is the satellite instrumental delay with respect to the satellite k and $b_{rj,Pi}$ is the receiver instrumental delays with respect to the receiver j, finally, mp_{Pi} represents the multipath plus receiver noise in the pseudorange measurement.

Next, the observation equation for the carrier-phase measurement can be formed as:

$$\Phi_i = \rho + c\cdot(dT - dt) + \lambda_i N_i - d_{ion,i} + d_{trop} + b^{s_k,\varphi_i} + b_{rj,\varphi_i} + mp_{\varphi_i} \quad (2)$$

where λ_i is the wavelength of the L1 ($\approx$19 cm), L2 ($\approx$24 cm) and L5 ($\approx$25 cm) carriers in distance units, N_i is the carrier-phase ambiguity. b^{s_s,φ_i} and b_{rj,φ_i} represent the satellite and receiver instrumental delays on each carrier-phase observable and mp_{φ_i} is the carrier phase multipath and the noise.

To obtain the pseudorange multipath plus noise observable, the geometry-free combination of the pseudorange and carrier-phase measurements at the same frequency was taken as:

$$P_i - \Phi_i = 2d_{ion,i} - N_i\lambda_i + B^{s_k}_{rj,Pi} - B^{s_k}_{rj,\varphi_i} + mp_{Pi} - mp_{\varphi_i} \quad (3)$$

where $B^{s_k}_{rj,Pi}$ is the satellite and receiver instrumental delays of pseudorange and $B^{s_k}_{rj,\varphi_i}$ is that of carrier-phase as:

$B^{s_k}_{rj,Pi} = [b^{s_k,P_i} + b_{rj,Pi}]$ and $B^{s_k}_{rj,\varphi_i} = [b^{s_k,\varphi_i} + b_{rj,\varphi_i}]$

We can rearrange eqn. (3) solving for the pseudorange multipath plus noise term, mp_{Pi}:

$$mp_{Pi} = (P_i - \Phi_i) - 2d_{ion,i} + N_i\lambda_i + B^{s_k}_{rj,Pi} - B^{s_k}_{rj,\varphi_i} + mp_{\varphi_i} \quad (4)$$

Note in eqn. (4) that the pseudorange multipath plus noise cannot be measured directly from the combination of pseudorange and carrier-phase measurements at the same frequency due to ionospheric delay, carrier-phase ambiguity, carrier-phase multipath plus noise and satellite and receiver instrumental bias.

The ionospheric delays on the two different frequencies can be related as:

$$d_{ion,2} = \gamma\cdot d_{ion,1} \quad (5)$$

$$d_{ion,5} = \xi\cdot d_{ion,1} \quad (6)$$

where $\xi = \frac{f_1^2}{f_5^2}$ and $\gamma = \frac{f_1^2}{f_2^2}$

and where f_1, f_2 and f_5 are the corresponding carrier frequencies of L1, L2 and L5.

By taking the difference between the carrier-phase measurements at two frequencies, for example L1 and L5, the ionospheric delay on L1 can be computed as:

$$d_{ion,1} = \left(\frac{1}{(\xi - 1)}\right)\begin{pmatrix} \Phi_1 - \Phi_5 + \lambda_5 N_5 - \lambda_1 N_1 \\ + b^{s_k,\varphi_5} - b^{s_k,\varphi_1} + b_{rj,\varphi_5} - b_{rj,\varphi_1} \\ + mp_{\varphi_5} - mp_{\varphi_1} \end{pmatrix} \quad (7)$$

By substituting the expression for the ionospheric delay as given by eqn. (7) into eqn. (4), the multipath plus noise in pseudorange can be formed as:

$$mp_{P_1} = P_1 - (1 + \frac{2}{\xi - 1})\Phi_1 + \left(\frac{2}{\xi - 1}\right)\Phi_5 + M_{15} + A_{15} + B_{rj,15}^{s_k} - B_{rj,P_1}^{s_k} \quad (8)$$

where mp_{P_1} includes multipath plus noise for carrier-phase, M_{15}, ambiguity term, A_{15}, satellite and receiver differential hardware delay term, $B_{rj,15}^{s_j}$, and satellite and receiver hardware delay for pseudorange, $B_{rj,P_1}^{s_k}$ as follow:

$$M_{15} = \left(1 + \frac{2}{\xi - 1}\right)mp_{\varphi_1} - \left(\frac{2}{\xi - 1}\right)mp_{\varphi_5} \quad (9)$$

$$A_{15} = \left(1 + \frac{2}{\xi - 1}\right)\lambda_1 N_1 - \left(\frac{2}{\xi - 1}\right)\lambda_5 N_5 \quad (10)$$

$$B_{rj,15}^{s_k} = \left(1 + \frac{2}{\xi - 1}\right)B_{rj,\varphi_1}^{s_k} - \left(\frac{2}{\xi - 1}\right)B_{rj,\varphi_5}^{s_k} \quad (11)$$

Since the carrier-phase multipath and noise terms are a fraction of a wavelength, the carrier-phase multipath and noise are over two orders of magnitude smaller than those of pseudoranges. With that level, carrier-phase multipath and noise, M_{15}, could be neglected. And the satellite and receiver instrumental bias for pseudorange, $B_{rj,P_1}^{s_j}$, and carrier-phase, $B_{rj,15}^{s_j}$, are more or less constant but slowly varying in time. If we assume those terms are absorbed by ambiguity term, finally mp_{P_1} in eqn. (8) can represent the pseudorange multipath plus noise as well as a bias term which is mainly caused by ambiguities as:

$$mp_{P_1} = P_1 - (1 + \frac{2}{\xi - 1})\Phi_1 + \left(\frac{2}{\xi - 1}\right)\Phi_5 + A_{15} \quad (12)$$

Performing similar operation for L5 C5, we can get the following equation with the same assumptions which we described in above eqn. (8) through (12):

$$mp_{P_5} = P_5 - (\frac{2\xi}{\xi - 1})\Phi_1 + \left(\frac{2\xi}{\xi - 1} - 1\right)\Phi_5 + A_{51} \quad (13)$$

where $A_{51} = \left(\frac{2\xi}{\xi - 1}\right)\lambda_1 N_1 - \left(\frac{2\xi}{\xi - 1} - 1\right)\lambda_5 N_5$

Note in the following sections that we used the term, MP1, for a multipath plus noise on L1 C_1 observable and the term, MP5, for that of L5 C_5 observable.

Satellite and receiver differential code bias (DCB)

To obtain ionospheric delays as well as DCB observables using dual-frequency WAAS data, we first take the difference between the WAAS L1 C_1 measurement and L5 C_5 measurement.

The observation equations of C_1 and C_5 from eqn. (1) can be described as:

$$C_1 = \rho + c \cdot (dT - dt) + d_{ion,1} + d_{trop} + b^{s_k,C_1} + b_{rj,C_1} + mp_{C_1} \quad (14)$$

$$C_5 = \rho + c \cdot (dT - dt) + d_{ion,5} + d_{trop} + b^{s_k,C_5} + b_{rj,C_5} + mp_{C_5} \quad (15)$$

By subtracting C_5 in eqn. (15) from C_1 in eqn. (14), the ionospheric delays on C_1 as well as DCB observable between C_1 and C_5 can be related as:

$$C_1 - C_5 = d_{ion,1} - d_{ion,5} + b^{s_k,C_1} - b^{s_k,C_5} + b_{rj,C_1} - b_{rj,C_5} + v_p \quad (16)$$

where $v_p = mp_{C_1} - mp_{C_5}$

We can introduce the differential code bias (DCB) between C_1 and C_5 as:

$$DCB_{C_1-C_5} = [b^{s_k,C_1} - b^{s_k,C_5} + b_{rj,C_1} - b_{rj,C_5}] \qquad (17)$$

Then using eqn. (6), we can get:

$$C_1 - C_5 = (1-\xi)\cdot d_{ion,1} + DCB_{C_1-C_5} + v_p \qquad (18)$$

Then, solving for $DCB_{C_1-C_5}$ as:

$$DCB_{C_1-C_5} = (C_1 - C_5) - (1-\xi)d_{ion,1} + v_p \qquad (19)$$

Note in eqn. (19) that the term, $DCB_{C_1-C_5}$ cannot be measured directly from the geometry-free combination of pseudorange measurements, C_1 and C_5 due to ionospheric delay on the C_1 observable. In general, the ionospheric delay as well the DCB in eqn. (19) are simultaneously estimated in a least square or Kalman filter process.

However, since WAAS broadcasts L1 C_1 ionospheric delays at predefined ionospheric grid points, the ionospheric delay term in eqn. (19) can be evaluated by using interpolated WAAS L1 C_1 ionospheric delays, I_{WAAS}, using closest three or four WAAS grid point delays at the computed ionospheric pierce point [WAAS MOPS, 2001].

So finally, by replacing the $d_{ion,1}$ in eqn. (19) with the I_{WAAS}, the $DCB_{C_1-C_5}$ can be related as:

$$DCB_{C_1-C_5} = (C_1 - C_5) - (1-\xi)\cdot I_{WAAS} + v_p \qquad (20)$$

TEST RESULTS AND ANALYSIS

In this section, we investigate the overall quality of the WAAS L5 signal by comparing the C/N_0 values provided directly by the receiver. The computed MP1 and MP5 observables are also compared. After that, we discuss the characteristics of the WAAS GEO satellite DCB and the possible benefit of using WAAS GEO ranging measurements in the positioning domain.

Carrier power to noise density ratio (C/N_0)

IS-GPS-200D [2003] and IS-GPS-705 [2005] indicate that the transmitted signal power of the GPS L5 signal could be 0.6 dBW higher than that of the L1 C1 signal (also see Table 2).

To see the differences in the transmitted power of the actual WAAS L5 signal versus the L1 signal, the observed C/N_0 values of L1 and L5 signals from both GEOs, PRN135 and PRN138 are illustrated in Figure 2.

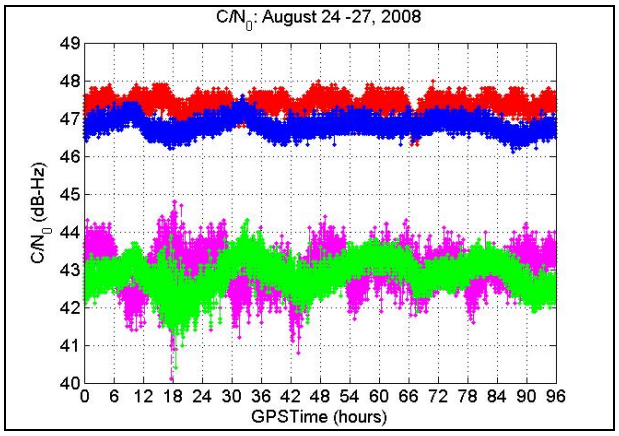

Figure 2. Carrier power to noise density ratio (C/N_0). The red dots represent the C/N_0 values for L1 signal for PRN138 and the blue dots show the L5 C/N_0 values for PRN 138. The magenta and green dots represent the L1 and L5 C/N_0 values, respectively for PRN135.

In Figure 2, we can first see that the overall C/N_0 values for the L1 and L5 signals from both GEOs, PRN135 and PRN138, are varying in time in the range of about ±1 dB-Hz. Those variations might be explained by neutral atmospheric effects or actual transmitted power fluctuations. By comparing the C/N_0 values between PRN138 and PRN135, we can also see that the C/N_0 values have clear elevation angle dependence. Also the C/N_0 values from the higher elevation angle GEO, PRN138, have smaller variations in time than those of PRN135.

The illustrated results in Figure 2 show that the observed WAAS L5 C/N_0 values are comparable with the L1 C/N_0 values for both GEOs. The compiled statistics of the observed C/N_0 values in the following Table 3 also shows that the C/N_0 values of the L1 and L5 signals are comparable.

Table 3: Statistics of the observed C/N_0 values for the WAAS GEOs, PRN135 and PRN138 for a four-day continuous period. (Units: dB-Hz)

SV	signal	Min	max	mean	std. dev
PRN138	L1	46.60	48.00	47.35	0.19
	L5	46.30	47.60	46.86	0.21
PRN135	L1	40.80	44.30	42.85	0.48
	L5	41.50	44.30	42.93	0.41

Code multipath and noise level (MP) analysis

In this sub-section, the multipath and noise level (MP) of C1 and C5 codes for both WAAS GEOs are analyzed. The MP observables referred to frequencies L1 and L5 were computed using the approach described above, equations (1) to (13).

In order to see a detailed view of each step of the computations, the step by step results are illustrated in Figure 3 and in Figure 4.

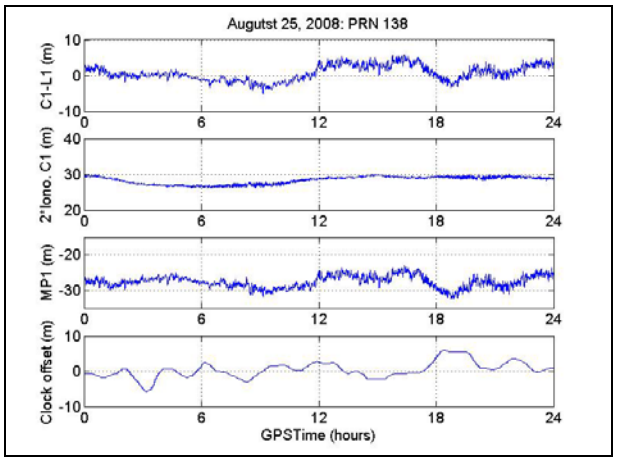

Figure 3. MP1 and related quantities for PRN138 on 25 August 2008. The y-axis range of all sub-plots is fixed to 20 m.

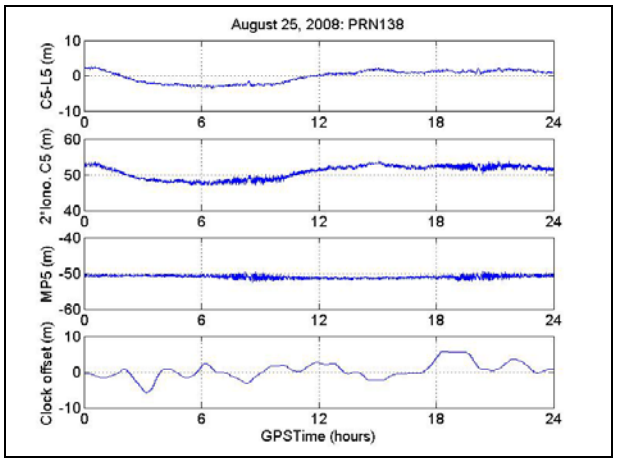

Figure 4. MP5 and related quantities for PRN138 on 25 August 2008. The y-axis range of all sub-plots is fixed to 20 m.

Figure 3 and Figure 4 show single day results of the computed MP1 and MP5 values for PRN138 on 25 August 2008. In the top panels, the C1-L1 observable and C5-L5 observable which contain two times the ionospheric delays, ambiguity, satellite and receiver differential code bias and combined carrier-phase and pseudorange MP values as described in the above eqn. (3) are illustrated and the compared results show that the noise level of the C1-L1 observable is higher than that of C5-L5 observable.

By comparing the second and third panels in Figure 4, we can see that the two-times ionospheric delay terms which are properly scaled to each observable C1 and C5 could be the main source of the low frequency time variations in the C5-L5 observable. After removing the ionospheric term, the remaining terms are only the constant ambiguity and slowly varying hardware delays, see eqn. (8) through (13). Therefore, the MP5 observable is more or less like a constant even though there exists a certain amount of bias which is caused by the carrier-phase ambiguities.

However, the MP1 observable in the third panel in Figure 3 shows different characteristics compared with the MP5 observable. The characteristics of the MP1 observable could be described as a constant bias which is caused by the ambiguity and MP effect and a specific pattern of unknown origin at the moment which is varying in time. If the carrier-phase ambiguities and the satellite and receiver DCB can be assumed as constant terms (see the third panels of the following Figure 8), the MP1 observable should behave like the MP5 observable. To see if there exists any correlation between the computed MP values and the GEO satellite clock offset which is provided by the WAAS GEO navigation message, correlation coefficients between the MP observables and the GEO satellite clock offsets were computed. The results show that the correlation coefficient between MP1 and GEO clock offset was -0.360 and it was -0.110 for the MP5. Those results show that there is a minor degree of correlation.

To see if the time-varying term in the MP1 observable is only observed on a specific day and if it also happened for the other GEO, PRN135, the MP1 and MP5 observables from both GEOs were computed for a continuous four day sample and are illustrated in Figure 5. In order to better illustrate the results, the mean of computed values was removed.

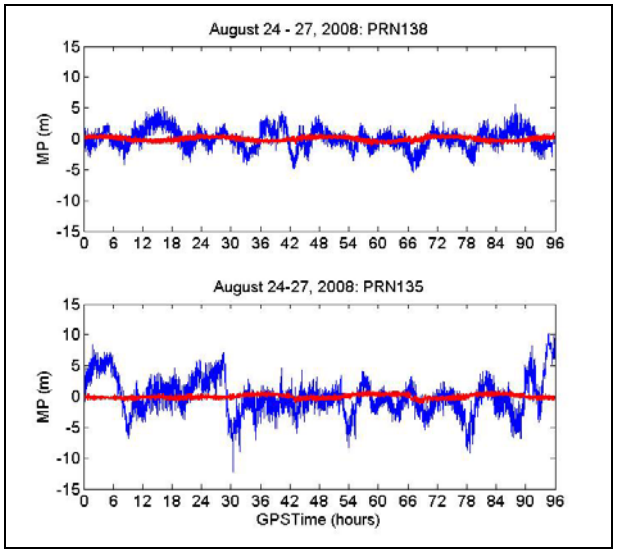

Figure 5. MP1 and MP5 observables from both PRN135 and PRN138 for a continuous four day sample, from 24 August 2008 to 27 August 2008. The blue dots indicate the MP1 observables and the red dots show the MP5 observables.

Figure 5 shows that the MP1 observables from both GEOs, contain a time-varying term which is not seen in the MP5 observables from both GEOs for the continuous four sample days.

However, the time-varying term in the MP1 observables have been identified as a contribution of the satellite DCB between C1 and C5 as discussed in the following section.

Since one of our purposes in this section is to see the overall performance of the new L5 C5 code compared to the L1 C1 code in terms of the noise level, a moving average filter was adopted to compute the final MP values in which the low frequency variations reduced. For the computation, cycle-slips in the carrier-phase measurements were identified first and the moving average filter applied to each separate arc with a window size of 10 measurements for both L1 C1 and L5 C5 codes.

The following Figure 6 shows the time series of the difference between the original and moving average filtered MP values for L1 C1 and L5 C5 codes for both GEOs.

In Figure 6, we can clearly see that the MP5 values have a better quality in terms of noise level compared with MP1 values. This is explained by the enhanced signal structure of the new L5 signals. The L5 C5 code has a higher chipping rate of 10.23 Mcps than the L1 C1 code of 1.023 Mcps, making the main peak in the cross-correlation function sharper by a factor of ten, and improving noise performance and mitigating the multipath effects [Enge, 2003].

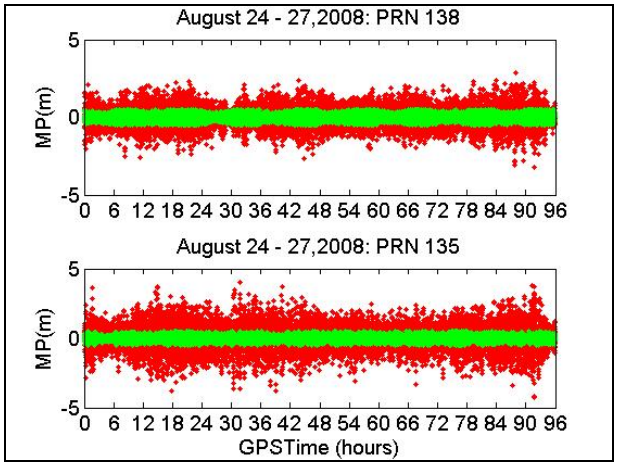

Figure 6. Difference between original and moving average filtered MP values for MP1 (red dots) as well as MP5 (green dots) for PRN135 and PRN138 from 24 August 2008 to 27 August 2008.

To see the overall performance of the L5 C5 code versus the L1 C1 code in terms of the noise level, the daily r.m.s. of the high-pass filtered MP1 and MP5 for the selected continuous four days were computed and are illustrated in Figure 7.

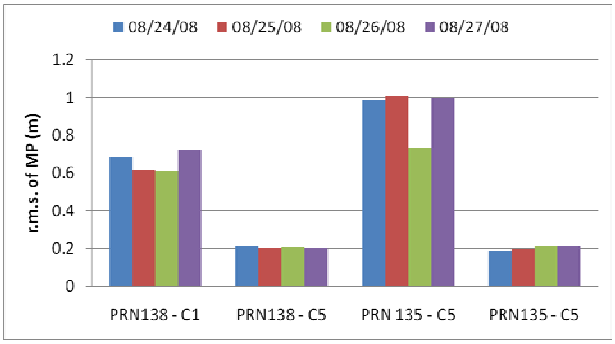

Figure 7, r.m.s. of the MP1 and MP5 for PRN135 and for PRN138 on four continuous days from 24 August 2008 to 27 August 2008.

In Figure 7, the r.m.s. of MP5 for both WAAS GEOs, show a better quality than that of MP1 as we expected. Since PRN135 was monitored at a lower elevation angle of 7.6° compared to that of 23.9° for PRN 138, the MP1 for the PRN135 was observed to be higher than that of PRN138.

However, interestingly, we observed that the r.m.s. of the MP5 values of PRN135 and PRN138 were comparable and the ranges of day-to-day variations were small. This might indicate the actual improvement of the enhanced signal structure for the WAAS L5 signals compared to the WAAS L1 C1 code.

Satellite & receiver differential code bias (DCB)

Since WAAS GEOs broadcast the dual-frequency, L1 and L5 data on the air, the ionospheric delays as well as satellite and receiver DCB should be estimated and compensated for when generating two independent signals, L1 and L5, which are uplinked to the GEOs.

To identify the overall behavior of DCBs in the GPS satellites and WAAS GEOs, we first generated the DCB observables for GPS PRN10 by use of the eqn. (14) through eqn. (20) on 25 August 2008. However, since GPS does not currently provide an L5 signal, the dual-frequency data, L1 C1 measurement and L2 P2 measurement were used to generate DCB observables.

However, note in this section that we also used the same term, DCB to represent the differential carrier-phase bias for a simplification.

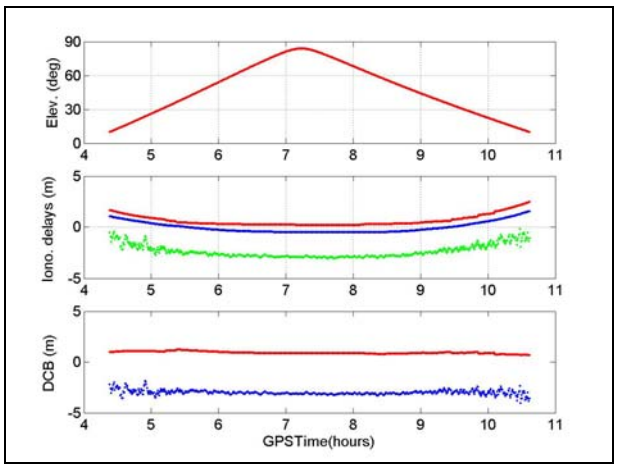

Figure 8. Computed satellite and receiver combined DCB for GPS PRN10 on 25 August 2008. The red dots in the second panel show the computed relative ionospheric delays by using L1 and L2 carrier phase measurements and the blue dots represent the ionospheric delays computed by using WAAS ionospheric corrections and the green dots show the computed ionospheric delays using C1 and P2 pseudorange measurements. The red dots in the third panel show computed carrier phase DCB and the blue dots show the computed pseudorange DCB.

Figure 8 shows the computed combined satellite and receiver DCB for the pseudorange measurements and the carrier-phase measurements for GPS PRN10 on 25 August 2008. Since PRN10 has few cycle slips on this day, and it therefore has a long arc with the elevation angle from 10° to about 85°, this satellite has been chosen to illustrate the DCB on GPS observations.

In the second panel, the observed slant ionospheric delays using pseudoranges are much noisier than those of carrier-phase measurements and also show that the noise level of the ionospheric measurements is elevation angle dependent as we expected. However, the overall variations of the observed pseudorange ionospheric delays in time are the same as those of the carrier-phase ionospheric measurements except for a residual bias which is caused by not fully accounting for the ambiguity in the carrier-phase measurements.

Since we used the WAAS ionospheric corrections as a reference to generate the DCB observables (see the equation (20)), the different DCBs for carrier-phase and pseudorange ionospheric measurements in the third panel could be generated. And the differences between carrier-phase DCB and pseudorange DCB in the third panel could be explained by the residual carrier-phase ambiguity as well as difference in the hardware delay bias between carrier-phase and pseudoranges observables. However, with this approach, it should be noted that the accuracy of the computed DCBs are dependent on the accuracy of the WAAS ionospheric corrections. The user ionospheric range errors (UIRE) [WAAS MOPS., 2001] for the WAAS ionospheric delay corrections varied from 0.3 m to 2.9 m for this satellite. With that accuracy, it might not be enough to precisely determine the different hardware delay biases between pseudranges and carrier-phases observables.

However, both computed DCBs using pseudorange and carrier-phase do not vary significantly in time indicating that the combined satellite and receiver bias is almost constant.

To take advantage of the precise but ambiguous carrier-phase ionospheric observables versus the unambiguous but less precise pseudorange ionospheric observables, the carrier-phase leveling technique was used [Komjathy, 1997]:

$$I_{comb_i} = I_{\varphi_i} - \frac{\sum_{j=1}^{n} P_j (I_{\varphi_j} - I_{P_j})}{\sum_{j=1}^{n} P_j} \qquad (21)$$

where i and j are indices for the ionospheric observables starting at the beginning of an arc, i=1,2, …, n with the total number of ionospheric measurements, n, used to compute the offset between the carrier-phase ionospheric observables and pseudorange ionospheric observables and I_{comb_i} is the combined ionospheric measurement between the carrier-phase ionospheric measurement, I_{φ_i}, and pseudorange ionospheric measurement, I_{P_i}. In general, the weight, P_j is determined based on an elevation angle

of the measurement at the specific epoch j. To compute the amount of leveling, twenty epochs (10 minutes) of data used.

And the final DCB values were computed based on those leveled ionospheric observables versus the WAAS ionospheric corrections (see the third panel in Figure 9).

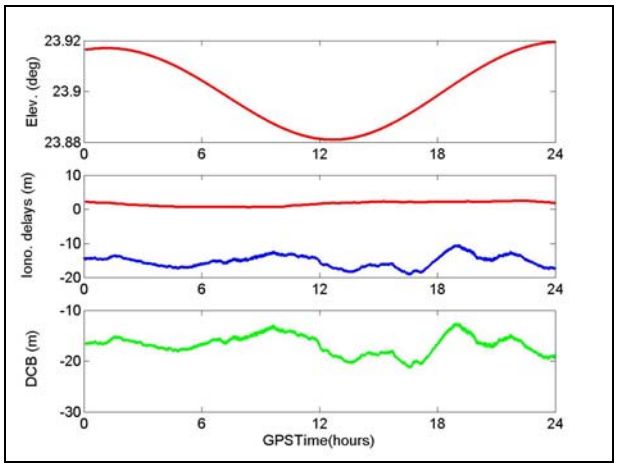

Figure 9. Computed satellite and receiver combined differential code bias (DCB) for WAAS PRN 138 on 25 August 2008. In the second panel, the red dots show the computed ionospheric delays using WAAS ionospheric corrections and the blue dots represent the carrier-phase leveled ionospheric delays.

In Figure 9, the top panel shows the elevation angle change over a day for PRN138. It shows that even though PRN138 is a geostationary satellite, there is some degree of movement. In the second panel, the leveled ionospheric delays could be identified as having more variations in time than the ionospheric delays computed from the WAAS corrections. And finally, the differences between leveled ionospheric delays and WAAS ionospheric delays were computed as DCB estimates and illustrated in the third panel.

To see if there is any correlation between estimated DCB values and the time variations which we observed in the WAAS MP1 observable, a correlation analysis has been conducted.

Since the receiver DCB is common for all the monitored satellites at UNB and observed as more or less constant in time as we saw in Figure 8, we took a mean of computed DCBs for all satellites and subtracted that value from the computed DCBs. In this case, the remaining term represents the variation of the satellite DCB versus the constant mean and which is illustrated in the first panel of the Figure 10. To compare the overall correlation between estimated DCB and MP1 at the same level, the mean bias of all the MP1 values is also removed and illustrated in the second panel of Figure 10.

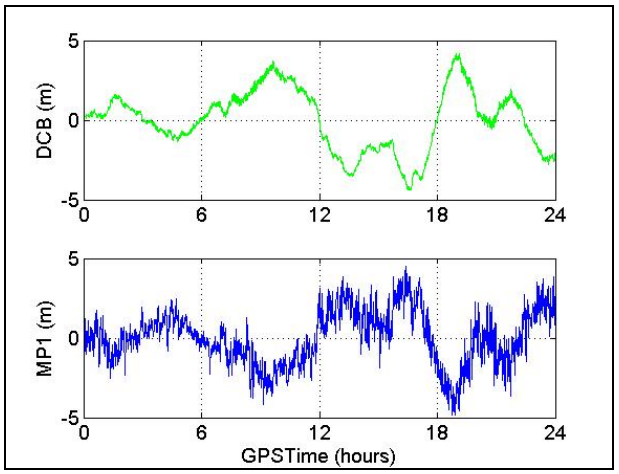

Figure 10. Correlation between estimated DCB and the WAAS MP1 for PRN138.

Finally, we can see that there is a strong anti-correlation between the variations of satellite DCB and the MP1 value. The correlation coefficient between the satellite DCB and the MP1 values was -0.856. WAAS currently does not provide the C1-C5 DCB value in the transmitted WAAS messages. However, if the WAAS satellites operated in the same way as GPS satellites, single frequency WAAS GEO ranging users would need the DCB value to resolve the clock referencing issue to use single frequency code observation for positioning. To circumvent this issue, it appears WAAS compensates for the C1-C5 bias in producing the L1 signal at the control segment. In this way, the single-frequency WAAS GEO ranging user does not need to consider the satellite DCB term.

Positioning domain results

To see if the C1-C5 satellite DCB have been compensated for producing WAAS GEO L1 C1 signals, the residuals from processing the C1 code for PRN138 in position-determination software have been analyzed. To process GPS plus PRN138 L1 C1 pseudoranges, the UNB WADGPS point positioning software [Rho and Langley, 2003 and 2005] has been used.

The overall processing scheme for the GPS plus PRN138 L1 C1 pseudorange is:

- WAAS satellite orbit and clock corrections were applied for GPS satellites: WAAS does not provide the GEOs orbit and clock corrections, above and beyond the GEO orbit and clock data in WAAS messages.
- WAAS ionosphere delay corrections have been applied for both GPS satellites and PRN138.

- UNB3 tropospheric delay model including Niell mapping functions used to mitigate the troposphere errors for both GPS satellites and PRN138.
- To account for receiver noise and multipath, an elevation angle dependent empirical stochastic model was used.

However, since the residual GPS orbit and clock errors (less than 1 m) and the WAAS GEO orbit and clock errors (more than 10 m based on GEO user range error (URA)) are different, different weighting schemes have been applied. For the GPS satellites, the initial GPS orbit error was set to 3 m (see UNB Website, [2008], the GPS orbit errors in these days are less than 2 m) but after WAAS orbit corrections for GPS satellites, residual errors are less than 1 m and it was 10 m for the PRN138. The GEO satellite accuracy of 10 m was determined based on the given GEO user range accuracy (URA) provided by the WAAS GEO navigation message and analyzing the positioning results. In most case, the URA index of the WAAS GEO satellites was 6 which indicated that the accuracy of GEO orbit is in the range of 13.65 m to 24.0 m [IS-GPS-200D]. However, the 10 m which was used for the positioning process was determined as a slightly optimistic minimum for the initial error which can make a best result in this setup of the point positing process.

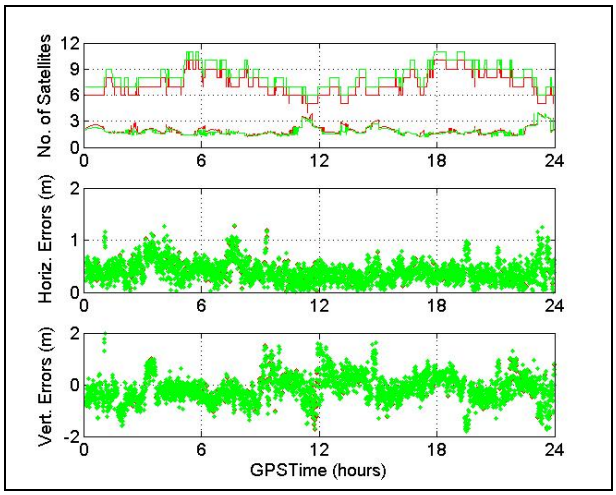

Figure 11. Benefit of using WAAS GEO ranging in point positioning. The top panel shows the number of satellites which have been used for the point positioning process and PDOP. The green trace shows the results of using GEO ranging data and the red trace shows the results without using WAAS GEO ranging measurements.

In Figure 11, the overall improvement of using the WAAS GEO satellite is negligible in the positioning results. The 95th percentile horizontal error was 0.783 m and the 95th percentile vertical error was 1.091 m when only the GPS measurements were used. When the GPS as well as the WAAS GEO PRN138 ranging measurements were used together, the 95th percentile horizontal error was the same and 1.087 m for the 95th percentile vertical error.

Those small effects in the positioning results by additionally using WAAS GEO ranging to the GPS measurements might be explained by the weight scheme that we used. Because of the low elevation angle of the PRN138 measurements with relatively less accurate GEO orbits than GPS, the weight of the GEO measurements was set to be much less than that of the GPS measurements. Therefore, the contributions of the WAAS GEO ranging measurements were not significant compared with the GPS measurements in this point positioning process for the particular data set used with a large number of GPS satellites observed.

However, as the first panel in Figure 11 shows, the benefit of using the WAAS GEO ranging measurements in the point positing process is in the improvement of dilution of precision (DOP) values. So it might be more beneficial to use WAAS GEO ranging measurements in more challenging situations where the number of monitored GPS satellites is quickly changing and/or fewer satellites are monitored as in a kinematic situation. Likely in such situations, there will also be better positioning results if both WAAS GEOs are used for positioning as well as GPS satellites.

To see the residual errors for WAAS PRN138 compared with those of GPS satellites, they are illustrated in Figure 12.

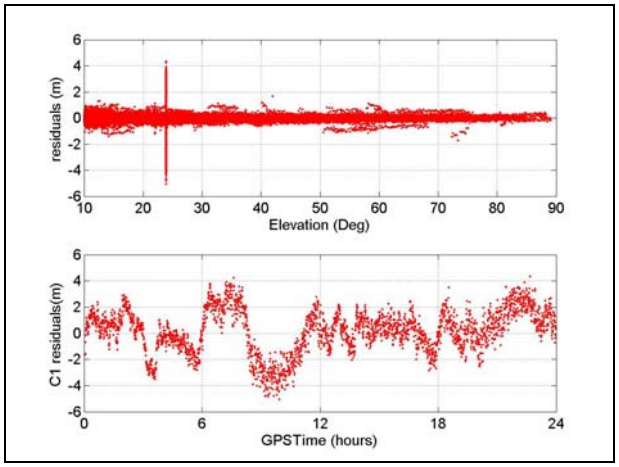

Figure 12. Residual errors for L1 C1 for PRN138 and GPS satellites (top panel) and PRN138 alone (bottom panel) on 25 August 2008.

The top panel in the Figure 12 shows all the residual errors for the GPS satellites as well as WAAS PRN138 versus elevation angle. The residual errors of PRN138 are displayed at about 24° elevation angle and show more than 4 times bigger residual errors than the residuals of

GPS satellites at the same elevation angle. Since the ionosphere and troposphere errors have been corrected, the dominant error sources are likely the residual GEO orbit and clock errors. The overall range of the residual error variations were observed at about ±4 m level. This figure indicates that a proper weighting scheme needs to be used for WAAS GEO range measurements in the positioning domain.

Finally, the second panel in Figure 12 shows the time series of the residual errors for PRN138. By comparing Figure 10 and Figure 12, we observed there are no strong correlations between the overall variation of the PRN138 residual errors and the estimated satellite DCB. The correlation coefficient between C1 residuals and the estimated satellite DCB was -0.165.

CONCLUSIONS

The quality of the new WAAS L5 signal has been evaluated by comparing selected signal quality indices for the L1 and L5 signals.

C/N_0 values for the WAAS GEOs, PRN135 and PRN138, have been compared on the L1 and L5 frequencies. The result showed that the signal strength of WAAS L5 is not stronger than L1 but rather reaches similar values, within ±1 dB-Hz, as those of the C/N_0 of the C1 code on the L1 frequency.

By comparing the multipath plus noise level between L1 C1 and L5 C5 codes, we found that the enhanced signal structure of the L5 has a better quality in terms of multipath plus noise level compared to the L1 C1 code.

Currently, the WAAS control segment is using dual frequency data from the GEOs. By examining the multipath plus noise and estimated DCB values, we found that WAAS GEO satellite DCBs appear to be varying in time and that the WAAS control segment compensates for the C1-C5 DCB bias when producing the L1 C1 signal.

The residual errors in the positioning domain results indicate that a proper weighting scheme should be used for incorporating WAAS GEO range measurements as additional to the GPS measurements in the positioning domain.

It should be pointed out that although WAAS currently transmits L5 signals, they are not intended for end users at this time.

ACKNOWLEDGMENTS

The research reported in this paper was supported by the Natural Sciences and Engineering Research Council of Canada and the GEOID Network of Centres of Excellence. The authors would like to thank NovAtel Inc. for allowing us to use their special firmware as well as for the receiver used in this research.

REFERENCES

Enge, Per (2003). “GPS Modernization: Capabilities of the New Civil Signals.” Invited Paper for the Australian International Aerospace Congress Brisbane, 29 July – 1 August.

Grewal, Mohinder S. (2008). “GNSS Solutions: WAAS Functions and Differential Biases.” InsideGNSS, Vol. 3, No. 4, May/June, pp. 18-23.

Hsu, Po-Hsin, L. Cheung and M. Grewal (2004). “Prototype Test Results of L1/L5 Signals of Future GEO Satellites.” Proceedings of ION GNSS 2004, 17th International Technical Meeting of the Satellite Division of The Institute of Navigation, Long Beach, CA, 21-24 September 2004, pp. 1359-1366.

Hsu, Po-Hsin, L. Cheung and M. Grewal (2007). “Method and Apparatus for Wide Area Augmentation System Having L1/L5 Bias Estimation.” United States Patent 20070067073, International Publication Date 5 April 2007.

IS-GPS-200D (2004). “NAVSTAR GPS Space Segment/Navigation User Interfaces.” GPS Joint Program Office, 7 December.

IS-GPS-705 (2005). “NAVSTAR GPS Space Segment/Navigation User Interfaces.” GPS Joint Program Office, Revision, IRN-705-003, 22 September 2005.

Komjathy, A. (1997). “Global Ionospheric Total Electron Content Mapping Using the Global Positioning System.” Ph. D dissertation, Department of Geodesy and Geomatics Engineering Technical Report No. 188, University of New Brunswick, Fredericton, Canada, 248 pp.

Rho, H., R.B. Langley, and A. Kassam (2003). "The Canada-Wide Differential GPS Service: Initial Performance." Proceedings of ION GPS/GNSS 2003, 16th International Technical Meeting of the Satellite Division of The Institute of Navigation, Portland, OR, 9-12 September 2003, pp. 425-436.

Rho, H. and R.B. Langley (2005). "Dual-frequency GPS Precise Point Positioning with WADGPS Corrections." Proceedings of ION GNSS 2005, 18th International Technical Meeting of The Institute of Navigation, Long Beach, CA, 13-16 September 2005, pp. 1470-1482.

Schempp, T. R. (2008). “Good, Better, Best: Expanding the Wide Area Augmentation System.” GPS World, Vol. 19, No 1, January, pp. 62-67.

UNB Website (2008): “GPS Broadcast Orbit Accuracy Statistics”, http://gge.unb.ca/gauss/htdocs/grads/orbit/. Accessed on September 6, 2008.

Van Dierendonck, A.J and C. Hegarty (2000), “
The New L5 Civil GPS Signal.” GPS World, Vol. 11, No.9, pp. 64-72.

WAAS MOPS (2001). “Minimum Operational Performance Standards for Global Positioning System/Wide Area Augmentation System Airborne Equipment.” RTCA Inc. Documentation No. RTCA/DO-229C, 28 November.